Low-lying excited-states and relaxation pathways of acetophenone

Attila Bende

Citation: AIP Conference Proceedings **1565**, 24 (2013); doi: 10.1063/1.4833689
View online: http://dx.doi.org/10.1063/1.4833689
View Table of Contents: http://scitation.aip.org/content/aip/proceeding/aipcp/1565?ver=pdfcov
Published by the AIP Publishing

Low-lying excited-states and relaxation pathways of acetophenone

Attila BENDE

Molecular and Biomolecular Physics Department, National Institute for Research and Development of Isotopic and Molecular Technologies, 65-103 Donath, 400293 Cluj-Napoca, Romania

Abstract. A numerical study is reported concerning the first and second singlet excited-states of acetophenone using the multireference self-consistent field (state-averaged CASSCF) method and tripla ζ basis set. The vertical excitation energies of low-lying excited-states were characterized using the SA-CASSCF method, as well as higher-level methods, such as CASPT2, MRCI and EOM-CCSD. The local minims and conical intersections found on the potential energy surfaces (PESs) were characterized in terms of molecular geometry and Mulliken population analysis. Different relaxation pathways on the PESs are identified and discussed.

Keywords: Acetophenone excited state; conical intersection; charge transfer; multireference methods
PACS: 31.15.A-;31.50.Df;33.25.+k

INTRODUCTION

Acetophenone (C6H5C(=O)CH3, AP) as the simplest aromatic ketone has become one of the classic aromatic carbonyl molecules for photochemical and spectroscopic studies. Due to the electronic excitation of the π electrons of the carbonyl group, electron charges can very easily migrate from the carbonyl fragment to the benzene ring and change the electronic structure of the aromatic ring. Aromatic carbonyl compounds differ from their aliphatic counterparts by exhibiting π electron conjugation between the aromatic and carbonyl groups, which influences the ordering of the n $\rightarrow \pi^*$ and $\pi \rightarrow \pi^*$ states, their photochemical reactivities, and the photodissociation mechanisms [1–3]. The electronic excited states of the acetophenone have already been studied by several authors. These theoretical works have mainly focused on vertical and adiabatic excitation energies [4] as well as on their photodissociation mechanisms [5], while theoretical studies on its nonradiative relaxation through the so-called conical intersections (CIs) are rather limited. With close-lying n $\rightarrow \pi^*$ and $\pi \rightarrow \pi^*$ excited states in both singlet and triplet manifolds AP is also ideally suited for the experimental study of the physical processes of intersystem crossing and phosphorescence, as well as photochemical reactions of valence isomerization, bond breakage, and atom transfer [6–8]. The gas phase absorption spectrum for AP in the region of 210–380 nm exhibits three broad peaks centered at 325, 273 and 230 nm, which are assigned to the $S_0 \rightarrow S_1$, $S_0 \rightarrow S_2$ and $S_0 \rightarrow S_3$ transitions, respectively [9].

In this work, we use high-level *ab initio* methods to re-evaluate the vertical and adiabatic excitation energies of the two lowest singlet excited states and to explore the possible relaxation mechanisms through non-radiative processes. At the same time we will also focus on the comparison of different excited state energies and geometries with those obtained for benzene and other aromatic molecular structures.

COMPUTATIONAL DETAILS

The geometry optimization calculations and the localization of conical intersections between surfaces of the different electronic states of AP have been performed at the state-averaged CASSCF level of theory using the Molpro computational chemistry program package [10]. For this case the triple ζ def2-TZVP basis set [11] was taken and no symmetry restrictions were considered for the molecular geometry.

If we neglect the Rydberg states, the lowest excited states of the AP are originated from the excitations of the valence π and lone pair n_O orbitals. Four π (one from C=O group of the carbonyl fragment and three from the benzene aromatic ring) and one n_O lone pair orbitals, from the oxygen atom, are located on the AP molecule. Thus an appropriate active space in CASSCF should include these five occupied orbitals with ten electrons. On the other hand, describing correctly the valence π excitation of the benzene molecule, according to Robb [12], we should consider at least three virtual orbitals in our active space. So, the final active space must contain four occupied orbitals, three virtual orbitals and eight electrons. The active space for the AP would be *(10,8)*, the nomenclature *(n,m)* denoting here an active space of *n* electrons and *m* orbitals. For the (10,8) active space, the number of configuration state functions (CSF) generated is 1176 while the number of Slater determinants is 3136.

In order to take into account the effect of electron correlations (static and dynamic) for the vertical excitation energies evaluation, we have performed further

Processes in Isotopes and Molecules (PIM 2013)
AIP Conf. Proc. 1565, 24-28 (2013); doi: 10.1063/1.4833689

calculations using higher-level methods: (i) multireference configuration interaction (MRCI) [13] with Davidson (D) correction [14], (ii) multi state second-order multireference perturbation theory (MS-CASPT2) [15], and (iii) equation-of-motion coupled-cluster theory for excited states (EOM-CCSD) [16–18]. For all these cases we used again the Molpro [10] software. In case of MS-CASPT2 calculations a level shift [19, 20] parameter of 0.2 was considered. For all multireference and single-reference CC2 [21] methods the first two electronic singlet excited states, S_1 and S_2, were accounted for. In case of CC2 method the Laplace Transformed Local CC2 version (LT-DF-LCC2) [22–24] with Density-Fitting [25–27] approximation was used together with the cc-pVTZ auxiliary basis set [28, 29] (JKFIT and MP2FIT). The molecular graphics (figures) were created using the Avogadro [30] software.

RESULTS AND DISCUSSION

As we have already mentioned in the previous section, the *ground state* optimized geometry structure of AP was obtained using the SA-MCSCF method with def2-TZVP basis set, considering the (10,8) active space configuration. Its geometry is shown in Figure 1. In case of the ground state geometry we found that the benzene ring showing a slight deviation from its value [31] in the perfect aromatic ring. The C–C bond distances are: 1.379 Å – 1.391 Å – 1.384 Å – 1.394 Å – 1.382 Å – 1.397 Å, respectively, while the C=O distance is 1.203 Å.

Vertical excitation energy. The vertical excitation energies up to the second excited level calculated with different theoretical methods are presented in Table 1. It

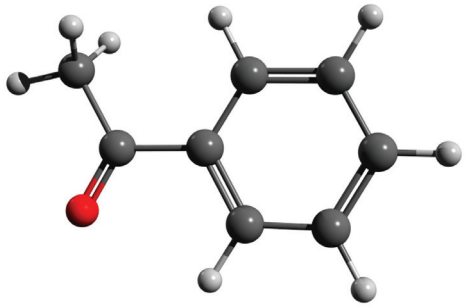

Figure 1. The optimized ground state geometry structure of the acetophenone

was found that the first excited state energy is close to 4.50 eV, while the second excited state energy is around 5.00–5.50 eV. These values are in good agreement with the experimental results [9]. Namely, for the first excited energy (n $\rightarrow \pi^*$ transition) the applied methods either at Hartree-Fock or electron correlation levels

Table 1. Vertical excitation energies (and their oscillator strength in parenthesis) for the two lowest excited states of AP and the benzene molecules.

	S_1 (eV)	S_2 (eV)
AP	$(n\pi^*)$	$(\pi\pi^*)$
SA-CASSCF(10,8)	4.52	5.60
	(0.0000)	(0.0091)
MS-CASPT2(10,8)	4.55	4.85
	(0.0001)	(0.0068)
MRCI (D) (10,8)	4.65	4.83
	(0.0001)	(0.0069)
EOM-CCSD	4.23	4.97
	(0.0001)	(0.0077)
LT-DF-LCC2	3.81	4.90
	(0.0000)	(0.0088)
Exp.	4.54	5.39
Benzene		
SA-CASSCF(6,6)	4.90	8.48
	(0.001)	(0.000)
MS-CASPT2(6,6)	5.10	6.93
EOM-CCSD	5.30	6.86
Acetone		
SA-CASSCF(4,4)	4.30	7.89
	(0.001)	(0.0139)
MS-CASPT2(4,4)	4.80	8.39
EOM-CCSD	4.51	7.63

give reasonable good values compared with the experimental result, while for the second excited state case ($\pi \rightarrow \pi^*$ transition), the electron correlation methods (MS-CASPT2, MRCI(D), EOM-CCSD, LT-DF-LCC2) give only a slightly lower energy values. The AP excited state can be more easily understood if one compare it with its constituent fragments of the benzene and acetone. The first two excited states of these constituent fragments are also presented in Table 1. Based on this comparison one can observe that the first excited state of the AP molecule is related to the first excites state of the acetone molecule, while the second excited state of the AP can be connected with the first excited state of the benzene. The symmetry of the electronic transition corresponds to the first excited state of the acetone ($n\pi^*$) as well as with the first excited state of the benzene ($\pi\pi^*$). In this way we have analyzed the charge redistribution for different excited states during the vertical excitation. Accordingly, we have found that in the case of the first excited state there is about 0.095e charge migration from the carbonyl fragment to the benzene one, while for the second excited state we have the opposite effect when about 0.086e charge leaves the benzene ring and appears as an extra charge at the carbonyl fragment. This different charge migration for the first and second excited state also demonstrate the nature of the excitation which was concluded before. Analyzing the magnitude of the oscil-

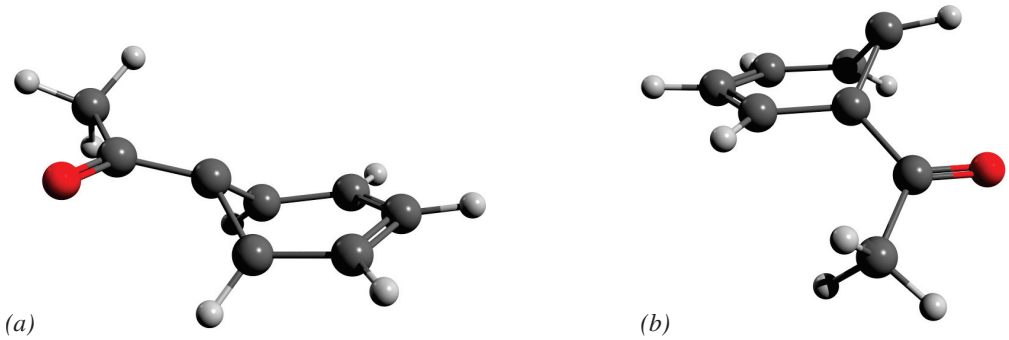

Figure 2. Two different conical intersection geometries between the ground and first excited state PESs

lator strength one was observed that the $S_0 \rightarrow S_1$ transition is a dark state and only the second excited state (S_2) can be reached via the vertical excitation. In this way is very interesting to see the relaxation pathways of the AP molecule without to include the dissociation of the fragments.

Equilibrium geometries. A critical issue for the laser-induced excitation of a molecule is to find, for the excited states, different stationary points on the potential energy surfaces (PES) and possible intersections between different PESs. For the beginning let us to analyze the equilibrium geometries for both excited state levels. The topology of the equilibrium structure of the first excited state is rather similar to the ground state geometry where only the C–C bonds of the benzene ring and the C=O double bond of the acetone fragment differs a little bit form the same values obtained for the ground state geometry. For this case the C–C bond distances are: 1.439 Å – 1.429 Å – 1.422 Å – 1.422 Å – 1.430 Å – 1.437 Å, respectively, while the C=O distance is 1.194 Å. The longest C–C bond distances are obtained for bonds neighbors with the C–C bond bridge which connects the benzene fragment with the carbonyl group (See Figure 1). As we can see, there is a more pronounced deviation from the perfect aromatic structure as one was obtained for the benzene ring in the ground state geometry. The reference energy of this stationary point is 4.54 eV obtained for CASSCF level of theory. This equilibrium geometry is also characterized by a different charge distribution. While in the vertical case we found 0.095*e* charge migration from the carbonyl fragment to the benzene, for the adiabatic case there is a small amount of 0.007*e* charge moves back from the benzene ring to the carbonyl fragment. As regards the spatial configuration of the atoms, the equilibrium geometry of the second excited state (where the S_0 equilibrium configuration was taken as the starting geometry) still keep the same arrangement as the ground or first excited states, namely the planar ring form. The difference is in the C–C bond lengths. For this case the C–C bond distances are: 1.457 Å – 1.416 Å – 1.372 Å – 1.404 Å – 1.448 Å – 1.458 Å, respectively, while the C=O distance is 1.222 Å. Here we can clearly identify two bonds with near double bond characters and other four bonds with single bond character. This equilibrium geometry of the benzene ring is rather different from the benzene ring behavior in other molecular complexes. We have found in case of 5-benzyluracil [32] that there is no any equilibrium structure with planar ring configuration for the benzene fragment before the system reaches the CI between the first and second excited state potential energy surfaces. The reference energy of this stationary point is 5.29 eV. In this case the picture of the charge redistribution is much more pronounced. While in the vertical case the benzene ring was positively charged (0.086*e* charge moved from the benzene ring to the carbonyl fragment), in the adiabatic case the benzene ring have an extra negative charge (-0.080*e*), which means that 0.19*e* charge moves back from the carbonyl group to the benzene ring.

Both the S_1 and S_2 equilibrium geometries are proper to benzene ring deformation. Besides of this ring deformation one would expect to have changes also on the carbonyl fragment. From our experience [32] the energy gradients of the vertical excitations prefer some well-defined directions, which in our case is the benzene ring deformation. In order to have geometry changes also at the carbonyl branch we have prepared a special starting geometry where the C=O bond was already enlarged closer to the single bond character. In this way we have obtained a new equilibrium geometry which shows significant deformations at the carbonyl part but also some C–C bond length changes at the benzene ring. The bond lengths are: for C–C bonds of benzene 1.416 Å – 1.366 Å – 1.392 Å – 1.386 Å – 1.371 Å – 1.414 Å, respectively, while the C=O distance is 1.389 Å. The position of the oxygen atoms almost coincides with the benzene plane, its dihedral angle is only 4.6°. The reference energy of this stationary point is 3.34 eV, which is lower with more

than 1 eV compared with the energy of the equilibrium geometry having the benzene aromatic ring changed. In this case 0.019*e* electron charge moves back from the carbonyl group to the benzene ring. Similarly, starting geometry optimization at the second excited state level from this slightly modified geometry configuration we obtain a new stationary configuration where the C=O bond is much more weakened than for the S_1 case. The bond lengths are: for C–C bonds of benzene 1.449 Å – 1.334 Å – 1.450 Å – 1.359 Å – 1.398 Å – 1.474 Å, respectively, while the C=O distance is 1.479 Å. For this case the reference energy is 6.05 eV which is higher with 0.76 eV than the previously obtained for stationary geometry on the S_2 PES.

Critical points on the PES. The critical points such CIs or avoided crossings (ACs) are very important from the point of view of the molecular relaxation (non-radiative) processes. The non-radiative relaxation pathways are built by geometry relaxation processes on the certain PES, then overcome different potential barriers and pass from one PES to another through the CIs and finally go down to the ground state geometry. For the transition between the ground and first excited states the benzene molecule has six equivalent geometries. In the AP case, being attached a carbonyl group to one of the carbon atoms from the benzene ring, the symmetry of these equivalent CI geometries is broken and appears different geometry configurations (See Figure 2) with slightly different energies (The reference energy is 5.17 eV for case *(a)* and 5.26 eV for *(b)*). Comparing these CI energies with the energy of the stationary points on the S_1 PES we can observe that there is no significant energy difference between the CI and that equilibrium geometry where we have found deformation only for the benzene ring configuration. If the geometry relaxation on the S_1 PES moves towards the carbonyl relaxation channel, there is a significant energy barrier for reaching the CI point from the stationary geometry.

CONCLUSIONS

A numerical study was reported concerning the first and second singlet excited-states of acetophenone using the multireference self-consistent field (state-averaged CASSCF) method and tripla ζ basis set. The vertical excitation energies of low-lying excited-states were characterized using the SA-CASSCF method, as well as higher-level methods, such as CASPT2, MRCI and EOM-CCSD. The results show that the first vertical excited state of the acetophenone shows similarity with the acetone's first excited state, while the second vertical excited state of the acetophenone has benzene character. The relaxation pathways of the acetophenone started from the second vertical excited state most probably follows the benzene ring relaxation mechanism. The study of higher order CI points and energy barriers exceeds the maximum length of this proceedings paper. More detailed study which includes the obtained CI geometries and the geometry of the triplet states are needed in order to have a global picture about the non-radiative processes in acetophenone.

ACKNOWLEDGMENTS

This work has been supported by the Romanian National Authority for Scientific Research (ANCS) through the PN-II-RU-TE-2011-3-0124 Research Project. I gratefully acknowledge to the Data Center of NIRDIMT Cluj-Napoca for providing computational infrastructure and technical assistance.

REFERENCES

1. W. H. Fang, D. L. Phillips, *ChemPhysChem* **3**(10), 889–892 (2002).
2. J. Li, F. Zhang, W. H. Fang, *J. Phys. Chem. A* **109**(34) 7718–7724 (2005).
3. Q. Fang, Y. J. Liu, *J. Phys. Chem. A* **114**(34) 680–684 (2010).
4. Y.-W. Wang, H.-Y. He, W.-H. Fang, *J. Mol. Struct. (Theochem)*, **634**, 281–287 (2003).
5. G. Cui, Y. Lu, W. Thiel, *Chem. Phys. Lett.* **537**, 21–26 (2012).
6. J. S. Feenstra, S. T. Park, A. H. Zewail, *J. Chem. Phys.*, **123**(22) 221104 (2005).
7. S. T. Park, J. S. Feenstra, A. H. Zewail, *J. Chem. Phys.*, **124**(17) 174707 (2005).
8. S.-H. Lee, K.-C. Tang, I-C. Chen, M. Schmitt, J. P. Shaffer, T. Schultz, J. G. Underwood, M. Z. Zgierski, A. Stolow, *J. Phys. Chem. A*, **106**(39) 8979–8991 (2002).
9. M. Berger, C. Steel, *J. Am. Chem. Soc.* **97**(17), 4817–4821 (1975).
10. MOLPRO, version 2012.1, A package of *ab initio* H.-J. Werner, P. J. Knowles, R. Lindh, F. R. Manby, M. Schütz, P. Celani, T. Korona, A. Mitrushenkov, G. Rauhut, T. B. Adler, *et al.* see `http://www.molpro.net`.
11. F. Weigend, R. Ahlrichs, *Phys. Chem. Chem. Phys.* **7**(18), 3297–3305 (2005).
12. I. J. Palmer, I. N. Ragazos, F. Bernardi, M. Olivucci, M. A. Robb, *J. Am. Chem. Soc.* **115**, 673–682 (1993).
13. P. J. Knowles, H.-J. Werner, *Theor. Chim. Acta* **84**(1-2), 95–103 (1992).
14. S. R. Langhoff, E. R. Davidson, *Int. J. Quant. Chem.* **8**(1), 61–72 (1974).
15. P. Celani, H.-J. Werner, *J. Chem. Phys.* **112**(13), 5546–5557 (2000).
16. H. J. Monkhorst, *Int. J. Quant. Chem.* **12**(S11), 421–432 (1977).
17. J. F. Stanton, R. J. Bartlett, *J. Chem. Phys.* **98**(9), 7029–7039 (1993).
18. T. Korona, H.-J. Werner, *J. Chem. Phys.* **118**(7), 3006–3019 (2003).

19. J. Lorentzon, M. P. Fulscher, B. O. Roos, *J. Am. Chem. Soc.* **117**(36), 9265–9273 (1995).
20. B. O. Roos, K. Andersson, *Chem. Phys. Lett.* **245**(2-3), 215–223 (1995).
21. O. Christiansen, H. Koch, P. Jørgensen, *Chem. Phys. Lett.* **243**(5-6), 409–418 (1995).
22. D. Kats, T. Korona, M. Schütz, *J. Chem. Phys.* **125**(10), 104106 (2006).
23. D. Kats, T. Korona, M. Schütz, *J. Chem. Phys.* **127**(6), 064107 (2007).
24. D. Kats, T. Korona, M. Schütz, *J. Chem. Phys.* **131**(12), 124117 (2009).
25. O. Vahtras, J. Almöf, M. V. Feyereisen, *Chem. Phys. Lett.* **213**(5-6), 514–518 (1993).
26. M. Schütz, *J. Chem. Phys.* **113**(22), 9986–10001 (2000).
27. M. Schütz, H.-J. Werner, *J. Chem. Phys.* **114**(2), 661–681 (2001).
28. F. Weigend, A. Köhn, C. Hättig, *J. Chem. Phys.* **116**(8), 3175–3183 (2002).
29. F. Weigend, *PhysChemChemPhys* **4**(18), 4285–4291 (2002).
30. M. D. Hanwell, D. E. Curtis, D. C. Lonie, T. Vandermeersch, E. Zurek, G. R. Hutchison, *J. Cheminformatics*, **4**, 17 (2012).
31. S. Xu, C. Wang and Y. Cui, *Chin. J. Chem.* **28**(5), 734–740 (2010).
32. M. Micciarelli, C. Altucci, B. Della Ventura, R. Velotta, V. Toşa, A. B. Gónzalez Pérez, M. Pérez Rodríguez, Á. R. de Lera, A. Bende, *Phys. Chem. Chem. Phys.* **15**, 7161 - 7173 (2013).